

# A preliminary design exploration of UAM vehicles

Sen Wang<sup>1</sup>, Lourenço T. Lima Pereira<sup>1</sup> and Daniele Ragni<sup>1</sup>

<sup>1</sup>Department of Flow Physics and Technology, Delft University of Technology  
*S.Wang-2@tudelft.nl*

## Abstract

This study presents a preliminary design exploration of Urban Air Mobility vehicles, based on a number of top-level aircraft requirements. The exploration focuses on designing a fully electric vertical takeoff and landing (eVTOL) vehicle that employs a conventional airframe coupled with tilted rotors. Using a low-fidelity design framework, a variety of configurations are facilitated by changing design variables such as operating speed, range, wing area/aspect ratio and number of propellers. The characteristics of these configurations are assessed by analysing the relation between power loading and disk loading. Additionally, operating expenses are evaluated to identify the most commercially viable design option. The investigation reveals that the considered architecture falls short for operations below a critical operating speed of 150 km/h, primarily due to the excessive reliance on propellers for lift generation. A configuration featuring a high aspect ratio wing and a larger number of propellers becomes preferable when operating at or above the critical speed, as the wing itself can produce sufficient lift. When operating above the critical speed, extending the operating range appears to lower operating expenses. Furthermore, noise levels during cruising are estimated to be significantly lower than during takeoff when operating at the critical speed or higher.

## 1 Introduction

Urban air mobility (UAM) is defined as an on-demand aviation service, projected to become viable in the air-taxi and air-metro markets in near future [1]. As an integral part of the Advanced Air Mobility (AAM) initiative, UAM aims to fill the voids left by conventional aviation industries[2] through the use of novel Vertical TakeOff and Landing (VTOL) vehicles. The concept focuses on facilitating flight operations within and around urban areas, primarily for the transportation of passengers and cargo. A growing interest in UAM is seen in recent years, driven by goals to alleviate traffic congestion and reduce fossil fuel consumption. A notable amount of research activities has been devoted to UAM, with studies covering perspectives including its safety, community acceptance, and economic feasibility [3, 4]. With the objective of improving versatility, control authority, while reducing emissions of exhaust gas and noise, electric propulsion systems are deemed more suitable for UAM operation [5, 6] than conventional thermal engines.

Despite growing interest, the adoption of electric powered eVTOL vehicles faces significant challenges due to the current state of battery technologies [7]. This issue mainly arises from the relatively low energy density of lithium-ion batteries, which is typically around 230-250 Wh/kg on cell level [8]. Hence, achieving an extended operating range may lead to an excessively heavy takeoff mass. Given the limitation, much of UAM developments focuses on intracity operations, with intercity and regional operations receiving comparatively less attention [9]. However, expected developments in the fields of batteries [10, 11] and electric motors [12] would make long distance operation more feasible in the coming decades. Hence, relevant research on regional operation will be beneficial.

To mitigate the energy density issue, the current strategy involves adopting an appropriate eVTOL architecture to minimize the energy consumption during UAM operation. Comparative analyses of eVTOL architectures indicate that a conventional airframe coupled with tilted rotors provides enhanced flexibility in improving vehicle performance for different operating ranges [13]. Contrary to multicopter architecture, this design employs a fixed wing to produce lift during cruising. The high-power demand is restricted primarily to mission phases such as takeoff/landing, climb/descent, and hovering. This approach effectively reduces energy consumption, thereby decreasing the necessary battery weight. Furthermore, this architecture offers more space for optimizing propeller

design, as tiltable rotors can be fully utilized across all mission phases, e.g., takeoff and cruising [13]. However, it's important to acknowledge that these advantages also come with certain drawbacks. For instance, the installation of a fixed wing increases the total weight of the vehicle. The rotor-tilting mechanism adds technical complexity and can lead to increases in both the size and weight of the powertrain [13].

In light of that, exploring the relevant design variables becomes crucial to identify the optimum configurations that can fulfill the intended mission objectives, while remaining economically competitive. In this study, a low-fidelity design framework developed at Delft University of Technology was employed to carry out a preliminary design exploration on UAM vehicles. The conceptual designs feature an architecture of conventional airframe coupled with tilted rotors. A set of design choices that impact the performance of UAM vehicle are considered to facilitate the conceptual designs. These are the operating range, cruise speed, number of propellers, and wing area. The lifting characteristics of the conceptual designs are assessed by analysing their relation between power loading and disc loading. Additionally, the operating expenses for each configuration are assessed. Following Brown and Harris [14], the assessment encompasses the pilot cost, maintenance cost, energy cost, and indirect operating cost. The quantified results is normalized with respect to the number of passenger and operating range, offering some insights for various business scenarios.

## 2 Methodology

In this study, the preliminary design exploration was carried out using a low-fidelity design framework developed at Delft University of Technology. The framework is based on analytical and semi-empirical methods, and its intended to facilitate a preliminary design process of eVTOL vehicles using a set of feasible Top-Level Aircraft Requirements (TLARs), the key mission requirements that drive the design activities. These TLARs are derived from assessment on operating scenarios and existing prototypes. [15]. In this section, the flow of design process is briefly introduced.

### 2.1 Preliminary design framework

The design process begins by defining the aforementioned TLARs. Using these inputs, a preliminary propulsion system is sized to meet the required operating conditions using actuator disk theory [16]. Subsequently, a first-order mass estimation of the vehicle is carried out through Roskam method [17]. The sizing process on propulsion system and first-order mass estimation iterates until convergence is reached in terms of the Maximum TakeOff Mass (MTOM) and total installed power.

In parallel to the aforementioned sizing process, the aerodynamic characteristics of the vehicle, e.g., coefficient of lift and drag etc., are estimated based on the viscous solution of XFOIL [18] and lifting-line theory [19]. Based on the results, an initial sketch of the UAM model that meets the revised mission requirements (derived from the first iterative sizing process) is created.

Following the aerodynamic characteristics of the vehicle, the design is enters another iterative process that encompasses the aerodynamic performance evaluation and second-order mass estimation [17]. At this stage, mass estimation at sub-system levels is progressively refined, and the corresponding aerodynamic performance is continuously updated and revised. The process converges when the determined cruising range meets the mission requirement.

In the end, the acoustic noise generated by operating UAM vehicle is evaluated, as noise emission is a critical factor in community acceptance of operating eVTOL vehicles in urban areas [20]. The tonal noise components are assessed through Hanson's model [21], based on the specifications of propulsion system and revised mission profile. Following the work of Fuerkaiti et al. [22], the emissions are computed over an imaginary sphere that covers the vehicle. The sphere is treated as a noise source, which allows for the prediction of the ground-level noise signature.

### 2.2 Design of experiments

In the context of this study, the TLARs are closely aligned with the mission definition and vehicle layout, encompassing operating range  $R$ , speed  $V$ , number of propellers  $N_{prop}$ , and wing area  $S$ . The range of  $R$  is draw from the market analysis conducted by NASA [23], and is set between 50 km to 200 km when considering a round trip for UAM and Regional Air Mobility (RAM) operations. A set of  $V$  is also considered as  $V$  governs the mission duration [23]. In reference to existing prototypes [13], the values of  $V$  are selected to be below 200 km/h in a conservative manner as it will largely affect the overall energy consumption. As previously mentioned, the conceptual

design features a fixed wing and tilted rotors, a number of  $N_{\text{prop}}$  and  $S$  are also considered. The corresponding values of aforementioned TLARs are summarized in table 1, and a total of 144 configurations are assessed. It should be noted that in this study, the modification of  $S$  is achieved by modifying the wing aspect ratio (AR) while keeping the wing span constant. The approach enables the assessment of vehicle aerodynamic performance without excessively increasing its footprint. A series of other design parameters need to be assumed for this top-level assessment. Following the design of Joby S4, with similar mission, architecture, and maximum range, wing span, fuselage dimensions, and propeller mounting are estimated.

$R$ [km]	$V$ [km/h]	$N_{\text{prop}}$	$S$ [m <sup>2</sup> ]	AR
50, 100, 150, 200	100, 150, 200	4, 6, 8, 10	11, 14, 19	6, 8, 10

Table 1: A summary of TLARs assessed for the design of experiments

As noted earlier, the state of battery and electric machine technology plays a significant role when assessing the eVTOL designs. In this exploration, we consider an entry into service (EIS) time of 2050, by which time the solid state battery technology is anticipated to be widely adopted. Corresponding assumptions are made based on technological projections of battery [10, 11] and electric motors [12]. For the electric motor, permanent magnet synchronous machines (PMSM) are considered. A summary of technological assumptions are presented in table 2.

Battery		Electric motor		
EIS	Energy density [Wh/kg]	Nominal c-rate [1/h]	Power density [kW/kg]	Mean efficiency [%]
2050	585	4	11.3	97

Table 2: A summary of technological assumptions

The lifting characteristics of the designs are evaluated by examining the relation between power loading and disk loading, as these values vary with changes in design variables. In this context, power loading is defined as the ratio between MTOM to the total installed power, while disk loading is defined as the ratio between MTOM and actuator disk area or thrust area. Power loading represents the hover lift efficiency, and is commonly observed to be inversely proportional to the disk loading [24]. Helicopters typically have a high power loading as they are characterized by extended duration of hover or near-hover flying. In general, lifting systems with high power loading exhibit low disk loading, and vice versa. A brief technical benchmark of the existing eVTOL vehicles agrees with this trend. Vehicles featuring a multicopter architecture, e.g., VoloCity and E-Hang 184, tend to have a smaller ratio of disk loading to power loading, compared to vehicles with tilttable ducted fans (Lilium Jets). In addition, this relation holds true across a wide range of lifting systems, encompassing helicopters and lift-fan vehicles (Fig. 3 of [13]). The power loading and disk loading of vehicles equipped with Tilt rotors/wings typically fall in approximate ranges of 2.4 kg/kW - 4.8 kg/kW and 50 kg/kW - 500 kg/kW, respectively [24].

A design filter, based on operating expenses (OE), is employed to identify the ideal configurations for various operating conditions, i.e., for different  $R$  and  $V$ . The OE is computed as the total operating expense divided by the number of passengers and  $R$ . As shown by Brown and Harris [14], OE consists of directing operating cost (DOC) and indirect operating cost (IOC). DOC can be further divided into pilot cost, maintenance cost, and energy cost. The pilot cost is estimated using an average wrap rate around €100/h, while the maintenance cost is evaluated using an approximate average wrap rate of €60/h [14]. Note the maintenance time is considered around 62.5% per flight hours [14]. The energy cost is approximated based on the average non-household electricity price (first half of 2023, European Commission), which is €0.1833/kWh. The value of IOC is then approximated to be 40% of DOC [14].

### 3 Preliminary Results

In this section, assessments on eVTOL design exploration are carried out, focusing on a set of design variables:  $V$ ,  $R$ ,  $S$ , and  $N_{\text{prop}}$ . For each operating speed  $V$ , the lifting characteristics of the designs are explored through investigating the relation between power loading and disk loading. The influence of the rest of design variables on this relation is analyzed. The operating expenses of the design configurations are evaluated to determine the commercially viable configurations for different operating ranges. In the end, the corresponding design configurations are shown and their noise emissions produced during takeoff and cruising are estimated.

### 3.1 Design exploration with $V = 100$ km/h

The relation between power loading and disk loading for the configurations design to operate at  $V = 100$  km/h is illustrated in Fig. 1, where the data points that correspond to  $R = 50$  km, 100 km, 150 km, and 200 km are depicted in color groups of red, green, blue, and yellow. Configurations with  $S = 11$  m<sup>2</sup>, 14 m<sup>2</sup>, and 19 m<sup>2</sup> are represented by squares, diamonds, and circles. To further enhance the visualization of increasing  $S$ , an increase in color saturation is employed. For structural strength considerations, a wing with a smaller  $S$  (higher AR) tends to be heavier compared to wings with larger  $S$  [17]. For the configurations with the same  $R$  and  $S$ , data points are connected in lines to demonstrate the variation in  $N_{\text{prop}}$ . Moving from left to right along the lines, the trend corresponds to a rise in  $N_{\text{prop}}$  and a decrease in total actuator disk area.

As illustrated in Fig. 1, the majority of connected points exhibit a pattern where power loading positively correlate with the disk loading. This trend suggests that increasing  $N_{\text{prop}}$  enhances propeller efficiency at the cost of increasing power demand. The result appears to contradict the typical inverse relation observed between power loading and disk loading for tilt-rotor vehicles [24]. The slope of lines become greater for missions with larger  $R$  and  $N_{\text{prop}}$ . A decrease in  $S$  is also observed to increase the slope. A comparative analysis of thrust generation during takeoff and cruising phases is then performed in aim to explain the trends. The result reveals that the propellers produce similar level of thrusts in both phases for most configurations, even though the wing contributes to lift generation while the vehicle is cruising. The observation suggests that, at a speed of  $V = 100$  km/h, the wing does not produce sufficient lift, resulting in a heavy reliance on the propellers for lift generation. As a consequence, a substantial portion of the vehicle's weight is attributed to the battery due to the high energy consumption. The benefit of wing installation is not effectively leveraged. In fact, the vehicle's lifting characteristics more closely resemble those of a multicopter architecture. The observed positive correlation between power loading and disk loading can be attributed to the joint effect of increasing  $R$ ,  $N_{\text{prop}}$ , and decreasing  $S$  since these variations collectively lead to the need for a heavier battery.

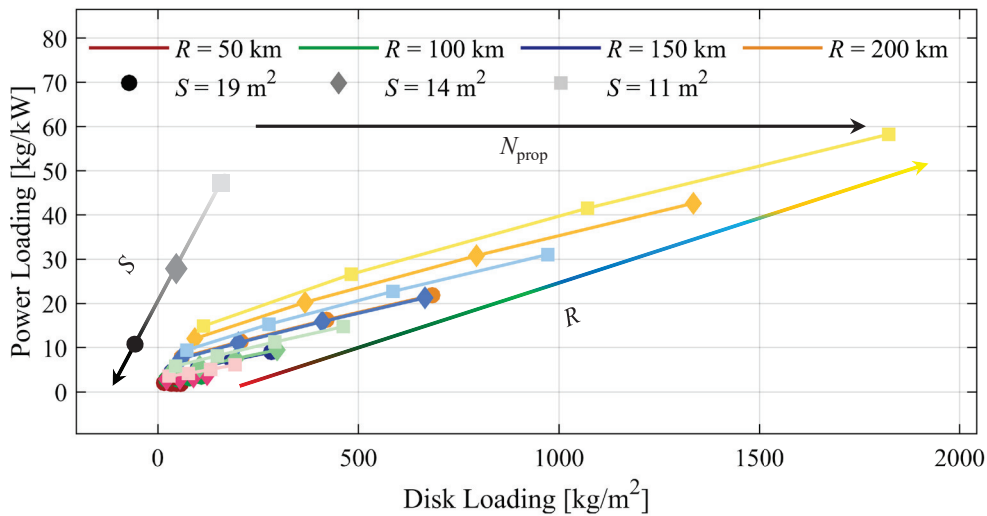


Figure 1: Power loading vs. disk loading with  $V = 100$  km/h

Next, the OE of all the design configurations are assessed to identify the ideal design for the intended mission. Following Fig. 1, the results of OE for configurations with different  $S$  are plotted against  $N_{\text{prop}}$  as shown in Fig. 2. The same scheme of color-coding used in Fig. 1 is employed here, where the configurations corresponding to  $R = 50$  km, 100 km, 150 km, and 200 km are depicted in red, green, blue, and yellow, respectively. The results reveal that for all intended missions, a larger  $S$  is in favor owing to its lighter weight. It is also found that a smaller  $N_{\text{prop}}$  is preferable despite increasing  $N_{\text{prop}}$  can reduce the weight of propulsion system [17]. Here, the benefit of having a lighter propulsion system is mostly offset by the increased power demand, which necessitates a heavier battery. This phenomenon becomes more apparent for extended operating range, as the slope of OE vs.  $N_{\text{prop}}$  grows larger with increasing  $R$ . It is also important to acknowledge that the current design exploration considers only a conventional gearbox for the powertrain. The advantage of increasing the number of propellers may be further compromised when the weight of a complex tilt-rotor system is considered.

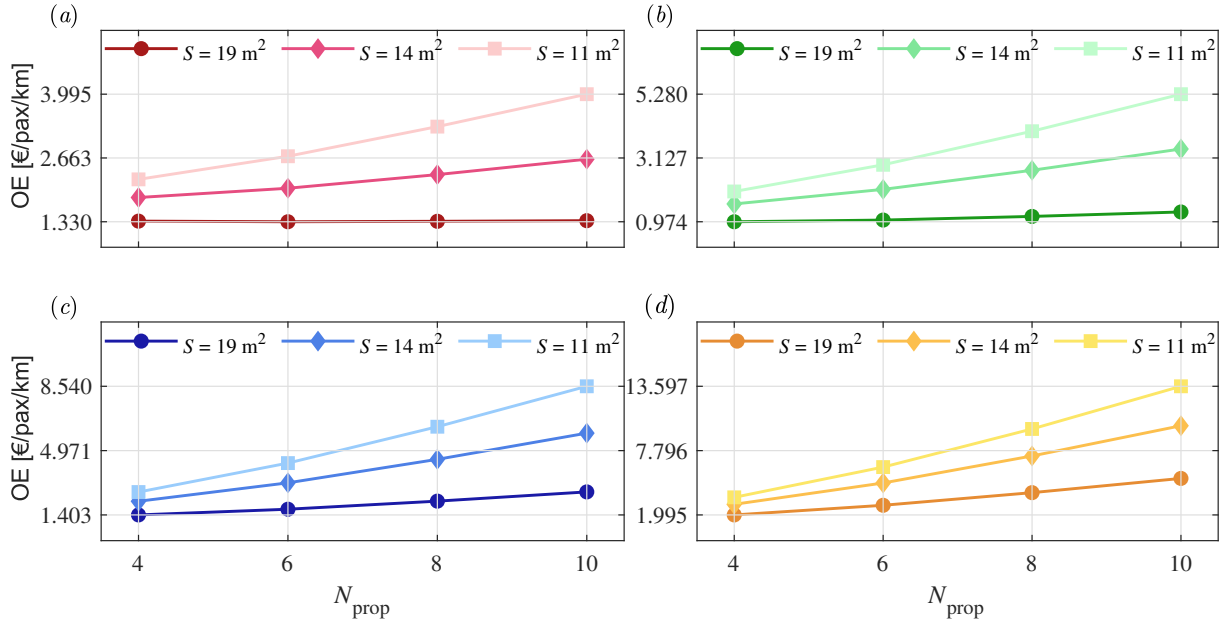


Figure 2: OE [€/pax/km] at  $V = 100$  km/h for  $R =$  (a) 50 km, (b) 100 km, (c) 150 km, and (d) 200 km

### 3.2 Design exploration with $V = 150$ km/h

The configurations designed for operating at  $V = 150$  km/h are assessed in this section. Following the aforementioned approach of analysis, the relation between power loading and disk loading is first investigated to assess the characteristics of the lifting systems. The results are demonstrated in Fig. 3, and the figure is annotated in the same manner as Fig. 1. A significant change in the pattern is seen when comparing Fig. 3 with Fig. 1. The configurations with a small  $S = 11$  m<sup>2</sup>, designed for extended range ( $R$ ), i.e. 150 km and 200 km, do not feature an inverse relation between power loading and disk loading. The pattern reflects that these configurations still exhibit heavy reliance on propeller for lift production, and is therefore akin to multicopters.

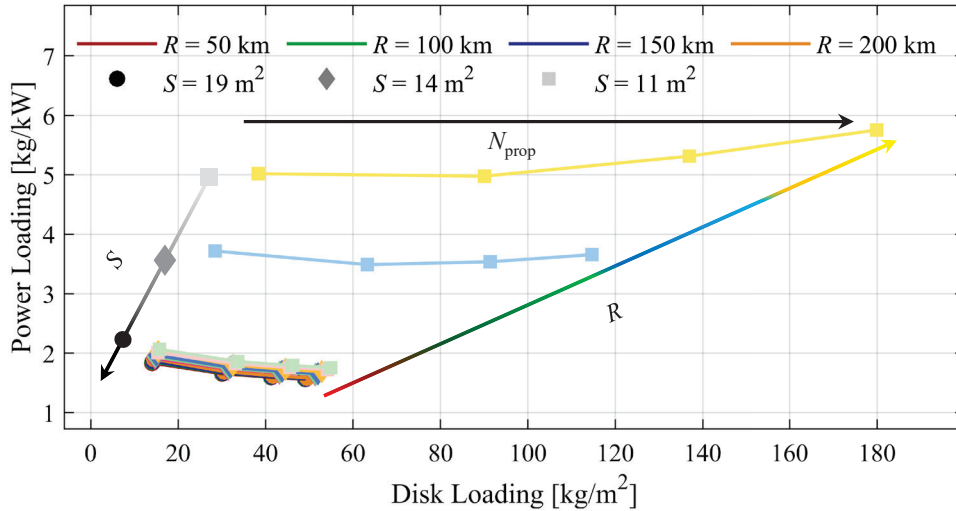


Figure 3: Power loading vs. disk loading with  $V = 150$  km/h

In addition to those configurations, it should also be noted that most of the configurations presented in Fig. 3 are observed at power loading  $< 3$  kg/kW. A zoom-in view is provided in Fig. 4 for further assessment on the relation between power loading and disk loading. The patterns associated with varying  $S$  and  $R$  are in agreement with those observed from Fig. 1, where a decrease in  $S$  and an increase in  $R$  contribute to increasing both power loading and disk loading. This is attributed to the fact that the corresponding variations in  $S$  and  $R$  both lead to a heavier

vehicle as previously explained. It is also found that an increase in  $N_{prop}$  corresponds to a rise in disk loading, but a reduction in power loading. Thus, a negative correlation is seen between power loading and disk loading, aligning with the trend identified for tilt-rotor vehicles [24]. Upon examining the thrust produced during cruising, it was found that numerous configurations still rely on propellers for lift support, especially for those design to operate at  $R = 150$  km and  $200$  km. However, this reliance is significantly less compared to that observed at  $V = 100$  km/h. The thrust required for cruising is near an order of magnitude smaller than that needed for takeoff. In addition, the weight of the propulsion system is reduced with increasing  $N_{prop}$ , leading to a lighter overall design. For a chosen lift-to-drag ratio of the intended mission, the aerodynamic drag experienced by the vehicle during cruising is reduced, indicating a lighter battery.

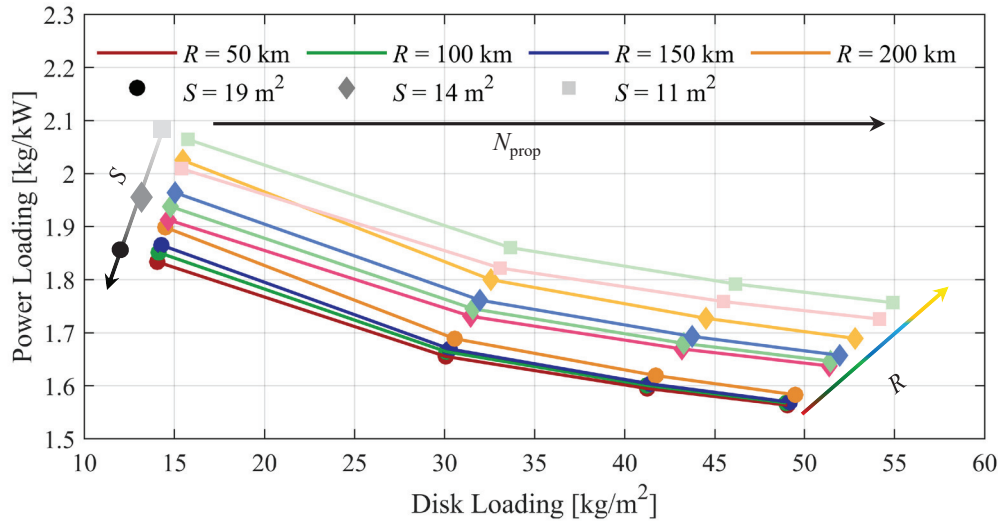


Figure 4: A zoom-in view of power loading vs. disk loading with  $V = 150$  km/h

The OE for those configurations presented in Fig. 4 is then assessed and the results are illustrated in Fig. 5. Note the configurations associated with  $S = 11$  m<sup>2</sup> for  $R = 150$  km and  $200$  km are not included here, as those designs more closely resemble multicopter vehicles and their OE is significantly higher than the rest.

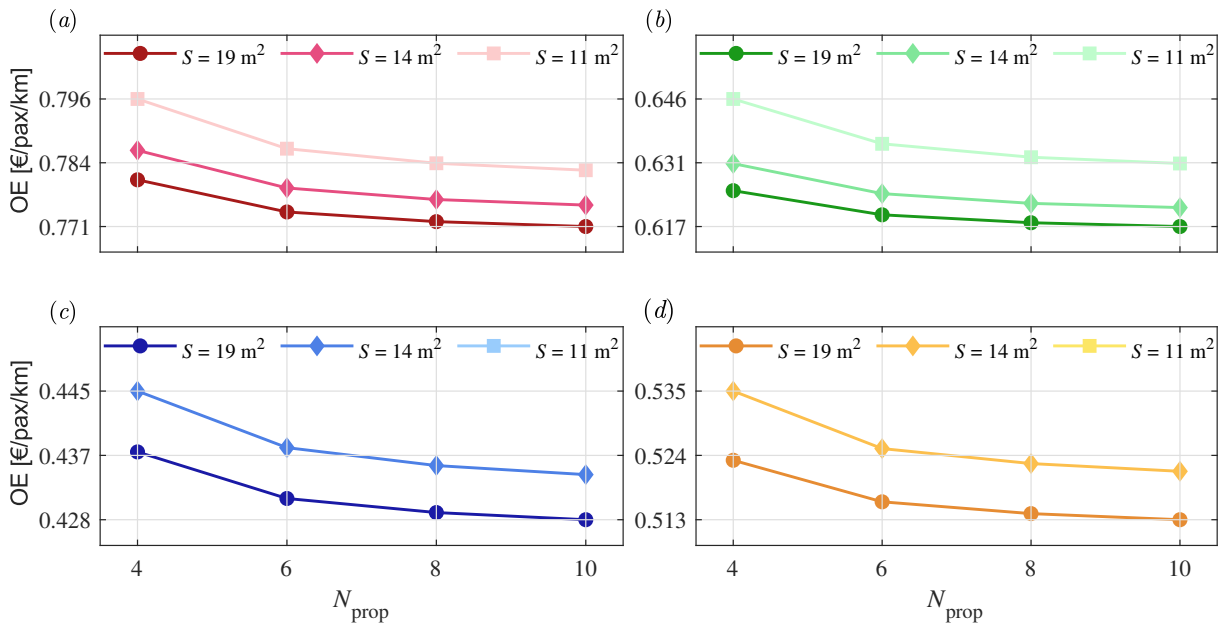


Figure 5: OE [€/pax/km] at  $V = 150$  km/h for  $R =$  (a) 50 km, (b) 100 km, (c) 150 km, and (d) 200 km

The observed trend show that a higher  $S$  is more advantageous for all evaluated  $R$ , as lift is proportional to



wing area. The dependence on propellers for lift support reduces when wing produces more lift. It is also seen that configurations with a higher  $N_{\text{prop}}$  tend to have a lower operating cost, attributing to its impact on cruising drag as mentioned earlier. The benefit of increasing the number of propellers gradually diminishes for  $N_{\text{prop}} > 10$ . Despite that, the level of OE stay below €1/pax/km for all the configurations that operate at  $V = 150$  km/h, which is significantly lower than the one observed from Fig. 2. The margin of OE due to modifying the design variables such as  $S$  and  $N_{\text{prop}}$  is much narrower in contrast to when operating at  $V = 100$  km/h.

### 3.3 Design exploration with $V = 200$ km/h

In the end, the configurations designed to operate at  $V = 200$  km/h are explored to assess the characteristics and performance of designs that operate at higher speed. The lifting characteristics of the vehicle is evaluated by probing the relation between power loading and disk loading, and the results are depicted in Fig. 6. The pattern observed here is similar to that of Fig. 4, where increases in both power loading and disk loading are associated with increasing  $R$  and decreasing  $S$ . As noted earlier, this is attributed to the extra weight introduced by extending the operating range and increasing AR. Furthermore, Fig. 6 reveals that an increase in  $N_{\text{prop}}$  leads to a decrease in power loading, but a rise in disk loading. As previously discussed, the former trend arises from a balance between the power-demand and cruising drag, influenced by varying  $N_{\text{prop}}$ . The latter result is associated with the reduction in thrust area as  $N_{\text{prop}}$  increases. Contrary to the scenario of operating at  $V = 150$  km/h, all the configurations explored in the current condition do not rely on propellers for lift generation, indicating wing is fully utilized for all intended  $R$  at  $V = 200$  km/h.

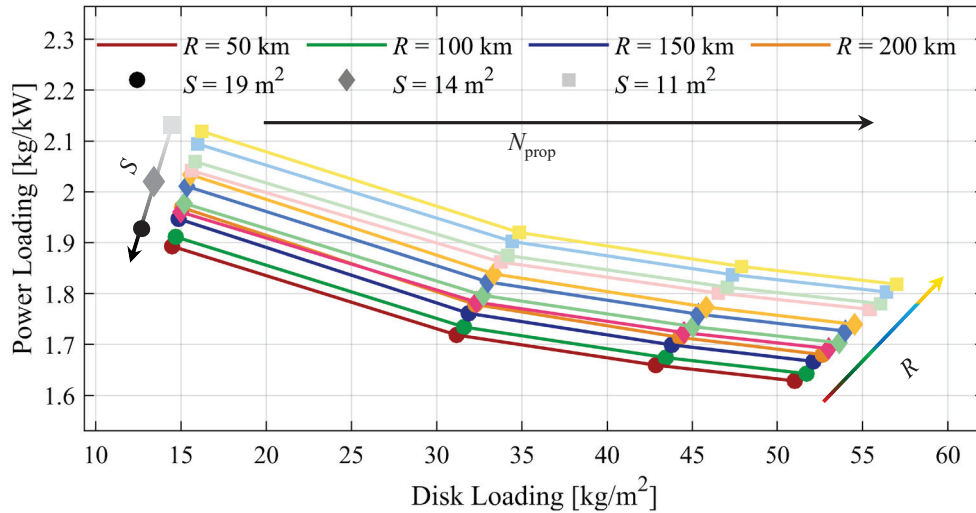


Figure 6: Power loading vs. disk loading with  $V = 200$  km/h

To identify the commercially competitive designs for each  $R$ , the corresponding OE is evaluated and the results are presented in Fig. 7. The results associated with varying  $N_{\text{prop}}$  matches the one observed in Fig. 5, where increasing the number of propellers appears to reduce OE. However, it is found that increasing  $S$  does not necessarily reduces OE when comparing to Fig. 5. The configurations designed for a shorter  $R$  tend to have a lower OE at  $S < 19$  m<sup>2</sup>. Given that the vehicles are designed to travel at the same speed, the mission time (man cost) is the same for the configurations with the same intended  $R$ . The difference in OE level is thereby attributed to variations in energy consumption. An inspection of cruising thrust proves this, as the observed pattern of thrust aligns with that of OE. The findings suggest that a smaller wing area corresponds to less cruising drag despite extra weight is introduced. This benefit is more pronounced for short-range missions at  $V = 200$  km/h.

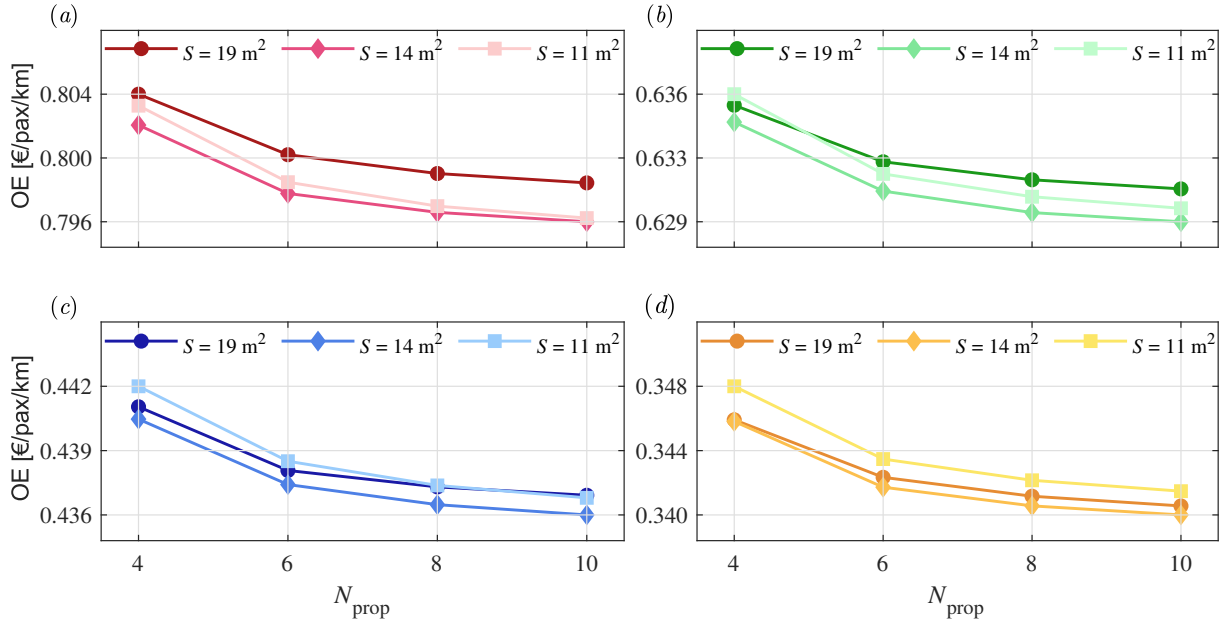


Figure 7: OE [€/pax/km] at  $V = 200$  km/h for  $R =$  (a) 50 km, (b) 100 km, (c) 150 km, and (d) 200 km

### 3.4 Discussion

The design filter based on OE identified the optimum configurations for each intended  $R$ , operating at different  $V$ . The design variables of these configurations are summarized in table 3. It is seen that configurations designed for slower speed and longer range favor a smaller  $S$  and  $N_{\text{prop}}$ , respectively. The level of  $\text{OE}_{\text{min}}$  of these configurations against  $R$  are presented in Fig. 8 to characterize the impact of  $R$  and  $V$  on the operating cost. The OE corresponding to speeds of 100 km/h, 150 km/h and 200 km/h are represented by dot-dash, dashed, and solid lines, respectively. Fig. 8 reveals that the level of OE at  $V = 100$  km/h is notably higher than at  $V \geq 150$  km/h. In concurrence with Moore [3], an adequate operating speed seems essential to fully capitalize on the aerodynamic benefit of wing installation. In the context of this study,  $V = 150$  km/h appears to be the critical speed based on the adopted assumptions. When the vehicle operates below the critical speed, extending the operating range beyond a certain point will increase OE. In contrast, a longer operating range is more favorable in terms of OE when the vehicle operates above the critical speed.

$V$ [km/h]	100			150			200		
$R$	$S$	$N_{\text{prop}}$	OE	$S$	$N_{\text{prop}}$	OE	$S$	$N_{\text{prop}}$	OE
[km/h]	[m <sup>2</sup> ]	-	[€/pax/km]	[m <sup>2</sup> ]	-	[€/pax/km]	[m <sup>2</sup> ]	-	[€/pax/km]
50	19	6	1.330	19	10	0.771	14	10	0.796
100	19	6	0.974	19	10	0.617	14	10	0.629
150	19	4	1.403	19	10	0.428	14	10	0.436
200	19	4	1.995	19	10	0.513	14	10	0.340

Table 3: A summary of ideal design variables for intended operating scenarios, defined by  $V$  and  $R$



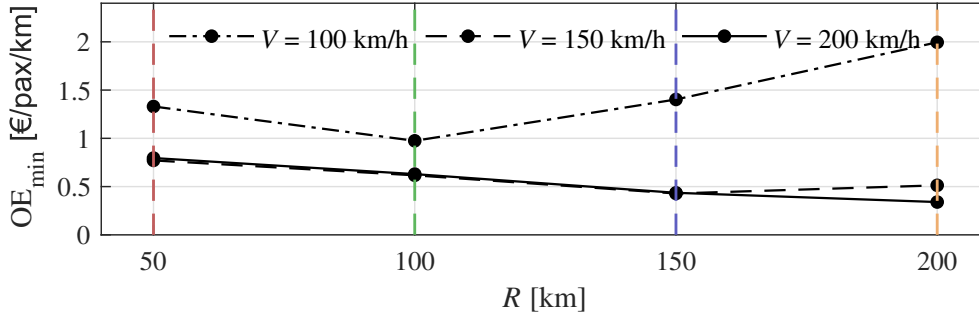


Figure 8:  $OE_{\min}$  [€/pax/km] for various  $V$

The sound power level of the ideal configurations during takeoff ( $PWL_T$ ) and cruising ( $PWL_C$ ) are estimated and the results are summarized in table 4. The results reveal that escalating the operating speed correspond to an increase in  $PWL$  for both takeoff and cruising phases. This is primarily due to the design choice favoring a greater number of propellers in configurations intended for high speeds. At  $V < 150$  km/h, the level of  $PWL_C$  converges to the level of  $PWL_T$  with increasing  $R$  as the vehicles resemble multicopter characteristics. When  $V$  is 150 km/h or higher, the noise level during cruising is estimated to be significantly lower than during takeoff, regardless of the range variation.

$V$ [km/h]	100		150		200	
$R$	$PWL_T$	$PWL_C$	$PWL_T$	$PWL_C$	$PWL_T$	$PWL_C$
unit	[km]	[dB]	[dB]	[dB]	[dB]	[dB]
50	135	37	138	30	162	37
100	123	60	139	32	163	37
150	131	85	141	34	164	37
200	139	103	142	36	165	38

Table 4: Sound power level ( $PWL$ ) during takeoff and cruising

## 4 Conclusion

In this investigation, a preliminary design exploration of the eVTOL vehicle is performed using a low-fidelity design framework. The architecture of eVTOL design is chosen as a tilt-rotor combined with a conventional airframe, a design choice aimed at fulfilling the mission requirements of both UAM and RAM operations. A range of design variables are altered to enable a systematic exploration of various conceptual designs, thereby providing a comprehensive analysis of the potential performance and capabilities of the eVTOL vehicle. It is crucial to emphasize that the results presented in this study are of a preliminary nature and are subject to future changes as the design algorithm and parameters undergo further refinement. Despite that, these preliminary findings are anticipated to offer valuable insights and guidance for UAM vehicle design.

Based on the preliminary assessment on operating conditions, it is determined that the eVTOL vehicles with a fixed wing are deemed inadequate to operate at a speeds lower than 100 km/h. The primary reason is that the wing does not produce sufficient lift to balance the weight of vehicle during cruising. Consequently, this necessitates reliance on propellers for lift generation during all mission phases, which increases the battery weight significantly. At low operating speed, it is apparent that the lifting characteristic of vehicle resembles that of a multicopter rather than the intended conventional airframe with tiltable rotor. The study reveals that the considered UAM vehicles need to operate at or above a critical speed to effectively utilize their wings. In the context of this investigation, the critical speed is determined to be 150 km/h. The analysis also indicates that operating below this speed results in notably higher operating expenses compared to speeds at or above 150 km/h. Extending the operating range is also shown to mitigate operational cost when the vehicle operates above the critical speed. The significance of operating speed is further highlighted in the noise estimation analysis. The results indicate that at lower speeds, the noise levels during takeoff and cruising tend to converge as the operating range increases. However, increasing the cruising speed to 150 km/h or higher effectively addresses the noise issue. This is achieved by reducing the reliance

on propellers for lift production. At these higher speeds, the estimated noise level during cruising is significantly lower than during takeoff, regardless of the operating range.

This investigation also assesses the influence of design variables, i.e., wing area/aspect ratio and number of propeller, on the performance of eVTOL vehicles. The impact of these design choices is found to be closely interconnected. The results suggest that reducing the wing area by increasing aspect ratio contributes to a heavier vehicle and lower lift production, although it may also result in reduced aerodynamic drag. Similarly, increasing the number of propellers tends to reduce the overall weight and size of propulsion system. However, the resulting configuration has a greater power demand, which may significantly increase the power consumption/battery weight. When the vehicle relies heavily on propeller to produce lift, the drawback of employing such propulsion system outweighs its benefit. Essentially, a design that incorporates a high aspect ratio wing and greater number of propeller is only in favor when the need to rely on propellers for lift production is minimal.

In the end, several intriguing findings have emerged from these preliminary results. For operations characterized by low operating speed and short operating range, a design that employs a multicopter architecture may be more suitable. This design offers advantages of efficient hovering capabilities, eliminating the need for wing and tail which can effectively reduce maximum takeoff mass. For operations that demand long-range capabilities, achieving a higher cruising speed is pivotal in counterbalancing the increase weight of battery.

## 5 Acknowledgement

This study is funded by the European Union under Grant Agreement No. 101097120. Views and opinions expressed in this study solely are those of the author(s) and do not necessarily represent those of the European Union or CINEA. Neither the European Union nor the Granting Authority can be held responsible for them.

## References

- [1] Anna Straubinger, Raoul Rothfeld, Michael Shamiyeh, Kai-Daniel Büchter, Jochen Kaiser, and Kay Olaf Plötner. An overview of current research and developments in urban air mobility – setting the scene for uam introduction. *Journal of Air Transport Management*, 87:101852, 2020.
- [2] Urban Air Mobility FAA. Concept of operations v1. 0. *US Department of Transportation Federal Aviation Administration, Washington DC*, 2020.
- [3] Mark D Moore. Concept of operations for highly autonomous electric zip aviation. In *12th AIAA Aviation Technology, Integration, and Operations (ATIO) Conference*, pages 1–15, 2012.
- [4] Giuseppe Palaia, Karim Abu Salem, Vittorio Cipolla, Vincenzo Binante, and Davide Zanetti. A conceptual design methodology for e-vtol aircraft for urban air mobility. *Applied Sciences*, 11(22):10815, 2021.
- [5] RK Ahluwalia, J-K Peng, X Wang, D Papadias, and J Kopasz. Performance and cost of fuel cells for urban air mobility. *International Journal of Hydrogen Energy*, 46(74):36917–36929, 2021.
- [6] Teresa Donato and Hasan Çınar. Conceptual design and sizing optimization based on minimum energy consumption of lift-cruise type e-vtol aircraft powered by battery and fuel cell for urban air mobility. In *Journal of Physics: Conference Series*, volume 2385, page 012072. IOP Publishing, 2022.
- [7] J Michael Vegh, Emilio Botero, Matthew Clark, Jordan Smart, and Juan J Alonso. Current capabilities and challenges of ndarc and suave for e-vtol aircraft design and analysis. In *2019 AIAA/IEEE Electric Aircraft Technologies Symposium (EATS)*, pages 1–19. IEEE, 2019.
- [8] Arumugam Manthiram, Yongzhu Fu, and Yu-Sheng Su. Challenges and prospects of lithium–sulfur batteries. *Accounts of chemical research*, 46(5):1125–1134, 2013.
- [9] Laurie A Garrow, Brian J German, and Caroline E Leonard. Urban air mobility: A comprehensive review and comparative analysis with autonomous and electric ground transportation for informing future research. *Transportation Research Part C: Emerging Technologies*, 132:103377, 2021.
- [10] Erik J Berg, Claire Villevieille, Daniel Streich, Sigita Trabesinger, and Petr Novák. Rechargeable batteries: grasping for the limits of chemistry. *Journal of The Electrochemical Society*, 162(14):A2468, 2015.

- [11] Taehoon Kim, Wentao Song, Dae-Yong Son, Luis K Ono, and Yabing Qi. Lithium-ion batteries: outlook on present, future, and hybridized technologies. *Journal of materials chemistry A*, 7(7):2942–2964, 2019.
- [12] Chrysoula L Pastra, Christopher Hall, Gokcin Cinar, Jon Gladin, and Dimitri N Mavris. Specific power and efficiency projections of electric machines and circuit protection exploration for aircraft applications. In *2022 IEEE Transportation Electrification Conference & Expo (ITEC)*, pages 766–771. IEEE, 2022.
- [13] P Nathen, A Strohmayer, R Miller, S Grimshaw, and J Taylor. Architectural performance assessment of an electric vertical take-off and landing (e-vtol) aircraft based on a ducted vectored thrust concept. *Lilium GmbH, Claude-Dornier StraeSSe, Weßling, Germany, Tech. Rep*, 2021.
- [14] Arthur Brown and Wesley L Harris. Vehicle design and optimization model for urban air mobility. *Journal of Aircraft*, 57(6):1003–1013, 2020.
- [15] Nicolas Peteilh, Thierry Klein, Thierry Y Druot, Nathalie Bartoli, and Rhea P Liem. Challenging top level aircraft requirements based on operations analysis and data-driven models, application to takeoff performance design requirements. In *AIAA Aviation 2020 Forum*, page 3171, 2020.
- [16] Albert Betz. *Introduction to the theory of flow machines*. Elsevier, 2014.
- [17] Jan Roskam. *Airplane design: Component weight estimation*. Roskam Aviation and Engineering Corporation, 1985.
- [18] Mark Drela and Michael B Giles. Viscous-inviscid analysis of transonic and low reynolds number airfoils. *AIAA journal*, 25(10):1347–1355, 1987.
- [19] Joseph Katz and Allen Plotkin. *Low-speed aerodynamics*, volume 13. Cambridge university press, 2001.
- [20] Stephen A Rizzi, Dennis L Huff, David D Boyd, Paul Bent, Brenda S Henderson, Kyle A Pascioni, D Caleb Sargent, David L Josephson, Mehmet Marsan, Hua Bill He, et al. Urban air mobility noise: Current practice, gaps, and recommendations. Technical report, 2020.
- [21] Donald B Hanson. Near-field frequency-domain theory for propeller noise. *AIAA journal*, 23(4):499–504, 1985.
- [22] Yunusi Fuerkaiiti, Damiano Casalino, Francesco Avallone, and Daniele Ragni. Aircraft community noise prediction in 3d environment using gaussian beam tracing. In *28th AIAA/CEAS Aeroacoustics 2022 Conference*, page 3079, 2022.
- [23] NASA Urban Air Mobility. Urban air mobility (uam) market study. *Retrieved the*, 30:2019, 2018.
- [24] Martin D Maisel. *The history of the XV-15 tilt rotor research aircraft: from concept to flight*. Number 17. National Aeronautics and Space Administration, Office of Policy and Plans . . . , 2000.